

Orbital selective Mott transition in multi-band systems: slave-spin representation and dynamical mean-field theory

L. de' Medici,^{1,2} A. Georges,¹ and S. Biermann¹

¹Centre de Physique Théorique, École Polytechnique 91128 Palaiseau Cedex, France

²Laboratoire de Physique des Solides, CNRS-UMR 8502, UPS Bâtiment 510, 91405 Orsay, France

We examine whether the Mott transition of a half-filled, two-orbital Hubbard model with unequal bandwidths occurs simultaneously for both bands or whether it is a two-stage process in which the orbital with narrower bandwidth localizes first (giving rise to an intermediate ‘orbital-selective’ Mott phase). This question is addressed using both dynamical mean-field theory, and a representation of fermion operators in terms of slave quantum spins, followed by a mean-field approximation (similar in spirit to a Gutzwiller approximation). In the latter approach, the Mott transition is found to be orbital-selective for all values of the Coulomb exchange (Hund) coupling J when the bandwidth ratio is small, and only beyond a critical value of J when the bandwidth ratio is larger. Dynamical mean-field theory partially confirms these findings, but the intermediate phase at $J = 0$ is found to differ from a conventional Mott insulator, with spectral weight extending down to arbitrary low energy. Finally, the orbital-selective Mott phase is found, at zero-temperature, to be unstable with respect to an inter-orbital hybridization, and replaced by a state with a large effective mass (and a low quasiparticle coherence scale) for the narrower band.

PACS numbers: 71.30+h, 71.10.Fd, 71.27.+a

I. INTRODUCTION

The Mott metal-insulator transition plays a central role in the physics of all strongly correlated electron materials. At a qualitative level, localization of the electrons can occur when the kinetic energy gain (typically given by the bare bandwidth) is smaller than the cost in on-site repulsive Coulomb energy (U). In recent years, dynamical mean-field theory (DMFT)^{1,2,3} has provided a consistent theoretical framework which has advanced our understanding of this phenomenon^{1,4}, in particular through the study of simplified models such as the one-band Hubbard model.

In real materials however, such as transition metal oxides, several orbital components are involved. Crystal-field effects and the Coulomb exchange energy (J) affect the energy of on-site atomic states, which no longer depend only on the total local charge as in the orbitally degenerate case. Furthermore, the inter-site hopping amplitudes can be significantly different for different orbital components (due e.g. to their relative orientations). It is therefore essential to understand how these effects can affect the Mott transition, and whether qualitatively new effects are possible when the orbital degeneracy is lifted.

Recently, this question has attracted a lot of attention. In their study of $\text{Ca}_{2-x}\text{Sr}_x\text{RuO}_4$, Anisimov *et al.*⁵ suggested that a partial localization could take place, in which some orbital components (with broader bandwidth) are conducting, while others (with narrower bandwidth) are localized (see also Ref.⁶). Following this proposal, several studies have been performed in the model context, with controversial results^{7,8,9,10,11}. Liebsch^{7,8,10} challenged the existence of such an ‘orbital-selective Mott transition’ (OSMT), on the basis of DMFT calculations, claiming that a single Mott transition always takes place for any value of the exchange coupling J .

Koga and coworkers^{9,11}, on the other hand, did find an OSMT within their DMFT calculations, and suggested that a unique transition is found only if $J = 0$. A symmetry argument was put forward to explain this finding.

In this paper, a clarification of this problem is attempted, using DMFT and another, complementary approach. The latter is based on a representation of fermion operators in terms of slave quantum spins, specifically forged to address multi-orbital models (Sec. III). A mean-field approximation based on this representation, similar in spirit to the Gutzwiller approximation, provides a fast and efficient method in order to investigate the Mott transition in a wide range of parameters (Sec. IV). In Sec. V, a detailed study of the previously unexplored regime in which one of the bands is much narrower than the other and $J = 0$ is presented, using exact diagonalizations and quantum Monte Carlo methods in the DMFT framework. Finally (Sec. VI), the effect of an inter-band hybridisation is considered.

II. MODEL

The model considered in this paper is a tight-binding model for two bands, coupled by local interactions. The Hamiltonian reads $H = H_0 + H_{int}$, where H_0 is the non-interacting part:

$$H_0 = - \sum_{m=1,2} t_m \sum_{\langle ij \rangle, \sigma} d_{im\sigma}^\dagger d_{jm\sigma} + \text{h.c.} + \sum_{i,m\sigma} (\epsilon_m - \mu) d_{im\sigma}^\dagger d_{im\sigma}, \quad (1)$$

in which $d_{im\sigma}^\dagger$ ($d_{im\sigma}$) creates (annihilates) an electron on the site i , in the orbital m , with spin σ . The ϵ_m 's are crystal-field levels and μ is the chemical potential, kept here for generality. In most of the paper however, we shall focus on the case of zero crystal-field splitting ($\epsilon_1 =$

$\epsilon_2 = 0$) and half-filling of each band (i.e one electron per site in each orbital, which corresponds to $\mu = 0$ given our normalization of the interaction term). At the end of the paper, we shall also consider the possibility of a non-zero inter-orbital hybridization.

The full interaction, in the case of degenerate bands in a cubic environment^{12,13} reads:

$$\begin{aligned} H_{int} = & U \sum_{im} \tilde{n}_{im\uparrow} \tilde{n}_{im\downarrow} + U' \sum_{i\sigma} \tilde{n}_{i1\sigma} \tilde{n}_{i2\sigma} \\ & + (U' - J) \sum_{i\sigma} \tilde{n}_{i1\sigma} \tilde{n}_{i2\sigma} \\ & - J \sum_i \left[d_{i1\uparrow}^\dagger d_{i1\downarrow} d_{i2\downarrow}^\dagger d_{i2\uparrow} + d_{i1\downarrow}^\dagger d_{i1\uparrow} d_{i2\uparrow}^\dagger d_{i2\downarrow} \right] \\ & - J \sum_i \left[d_{i1\uparrow}^\dagger d_{i1\downarrow}^\dagger d_{i2\uparrow} d_{i2\downarrow} + d_{i2\uparrow}^\dagger d_{i2\downarrow}^\dagger d_{i1\uparrow} d_{i1\downarrow} \right], \quad (2) \end{aligned}$$

where $\tilde{n}_{im\sigma} \equiv n_{im\sigma} - 1/2$. Following Castellani et al.¹², the reduction of the Coulomb interorbital Coulomb interactions U' as compared to the interorbital U is related to the Hund's coupling J by:

$$U' = U - 2J \quad (3)$$

In the case of vanishing Hund's rule coupling $J = 0$ the interaction vertex ($= U(n_1 + n_2 - 2)^2/2$) thus depends only on the total charge, while if $J \neq 0$ the inter-orbital interaction is weaker than the intraorbital one and becomes sensitive to the spin configuration.

III. SLAVE-SPIN MEAN-FIELD THEORY

A. Slave-spin representation

In this section, we introduce a new representation of fermion operators in terms of constrained (“slave”) auxiliary fields, which proves to be particularly convenient in order to study the multi-orbital hamiltonian above. The main idea at the root of any slave-variable representation is to enlarge the Hilbert space and to impose a local constraint in order to eliminate the unphysical states. When the constraint is treated on average, a mean-field approximation is obtained. Different slave-field representations will lead to different mean-field theories. The quality of the mean-field approximation can be improved by tailoring the choice of slave fields to the specific problem under consideration. In general, a compromise has to be found between the simplicity of the representation, the number of unphysical states which are introduced and the possibility of an analytical treatment of the resulting mean-field theory.

For finite- U Hubbard models, Kotliar and Ruckenstein¹⁴ have introduced a slave-boson representation which can be used in the present context, when appropriately generalised to multi-orbital models (in the spirit of the Gutzwiller approximation¹⁵). However, this method introduces many variational

parameters. On the opposite, S.Florens and one of the authors introduced a very economical representation of the N-orbital Hubbard model with $SU(N)$ symmetry based on a single slave variable, taken to be the phase conjugate to the total charge on a given lattice site (slave rotor representation)^{16,17}. However, this method is not appropriate when the orbital symmetry is broken, as in the present work.

Here, we introduce a new slave-variable representation²⁴ especially suited for dealing with multiband models, and addressing orbital-dependent properties. The basic observation behind this scheme is that the two possible occupancies of a spinless fermion on a given site, $n_d = 0$ and $n_d = 1$, can be viewed as the two possible states of a spin-1/2 variable, $S^z = -1/2$ and $S^z = +1/2$. This representation has been widely used in the case of hard-core bosons. In the fermionic context however, one needs to insure anticommutation properties, and this is done by introducing an auxiliary fermion f , with the additional local constraint:

$$f^\dagger f = S^z + \frac{1}{2} \quad (4)$$

In this manner, one obtains a faithful representation of the Hilbert space, which reads:

$$|0\rangle = |n_f = 0, S^z = -1/2\rangle \quad (5)$$

$$|1\rangle \equiv d^\dagger |0\rangle = |n_f = 1, S^z = +1/2\rangle \quad (6)$$

This constraint eliminates the two unphysical states $|n_f = 0, S^z = +1/2\rangle$ and $|n_f = 1, S^z = -1/2\rangle$. This representation is easily extended to the multi-orbital case, by treating each orbital and spin species in this manner. Hence a set of $2N$ spin-1/2 variables $S_{m\sigma}^z$ and auxiliary fermions $f_{m\sigma}$ are introduced ($m = 1, \dots, N$ is the number of orbitals), obeying the local constraint on each site:

$$\hat{n}_{im\sigma}^f = S_{im\sigma}^z + \frac{1}{2}, \quad (7)$$

This constraint can e.g be imposed with Lagrange multipliers fields $\lambda_{im\sigma}(\tau)$.

We now explain how to rewrite the original hamiltonian (1,2) in terms of the slave spins and auxiliary fermions. We consider first for simplicity the case $J = 0$, since the case $J \neq 0$ requires an additional approximation, as discussed later. For $J = 0$, the interaction involves only the total electron charge on a given site, and therefore reads:

$$H_{int}^{J=0} \equiv \frac{U}{2} \sum_i \left(\sum_{m,\sigma} \tilde{n}_{im\sigma} \right)^2 = \frac{U}{2} \sum_i \left(\sum_{m,\sigma} S_{im\sigma}^z \right)^2 \quad (8)$$

In order to express the non-interacting part of the hamiltonian, we need to choose an appropriate representation of the creation operator of a physical electron, $d_{im\sigma}^\dagger$. There is some freedom associated with this, since different operators in the enlarged Hilbert space spanned

by the slave-spin and auxiliary fermions can have the same action on the physical (constrained) Hilbert space. We have not used the obvious possibility $d^\dagger \rightarrow S^+ f^\dagger$, $d \rightarrow S^- f$. This representation is correct in the physical Hilbert space (i.e when the constraint is treated exactly), but it can be shown that additional mean-field approximations based on this representation will ultimately lead to a problem with spectral weight conservation because S^+ and S^- do not commute. Instead, we have chosen the representation $d^\dagger \rightarrow 2S^x f^\dagger$, $d \rightarrow 2S^x f$, which is identical to the previous one on the physical Hilbert space, and involves commuting slave-spin operators. With this choice, the non-interacting part of the hamiltonian reads:

$$H_0 = - \sum_m t_m \sum_{\langle ij \rangle, \sigma} 4S_{im\sigma}^x S_{jm\sigma}^x (f_{im\sigma}^\dagger f_{jm\sigma} + h.c.) + \sum_{i,m\sigma} (\epsilon_m - \mu) f_{im\sigma}^\dagger f_{im\sigma}$$

At this stage, no approximation has been made, provided the constraint is treated exactly.

B. Mean-field approximation

Approximations will now be introduced, which consists in three main steps: i) treating the constraint on average, using a static and site-independent Lagrange multiplier $\lambda_{m\sigma}$ ii) decoupling the auxiliary fermions and slave-spin degrees of freedom, and finally iii) treating the slave-spin hamiltonian in a single-site mean-field approach. This last step is quite independent of the two previous ones, and can be rather easily improved on, as done in¹⁷.

After the first two steps, one obtains two effective hamiltonians:

$$H_{eff}^f = - \sum_m t_m^{eff} \sum_{\langle ij \rangle, \sigma} (f_{im\sigma}^\dagger f_{jm\sigma} + h.c.) + \sum_{i,m\sigma} (\epsilon_m - \mu - \lambda_m) f_{im\sigma}^\dagger f_{im\sigma} \quad (9)$$

$$H_{eff}^S = - \sum_m 4J_m^{eff} \sum_{\langle ij \rangle, \sigma} S_{im\sigma}^x S_{jm\sigma}^x + \sum_{i,m\sigma} \lambda_m (S_{im\sigma}^z + \frac{1}{2}) + H_{int}[\{\vec{S}_{im\sigma}\}] \quad (10)$$

with $H_{int}[\{\vec{S}_{im\sigma}\}] = U/2 \sum_i (\sum_{j \neq i} S_{jm\sigma}^z)^2$ for $J = 0$. In these expressions, t_m^{eff} and J_m^{eff} are effective hoppings and slave-spin exchange constants which are determined from the following self-consistency equations:

$$t_m^{eff} = 4t_m \langle S_{im\sigma}^x S_{jm\sigma}^x \rangle \quad (11)$$

$$J_m^{eff} = t_m (f_{im\sigma}^\dagger f_{jm\sigma} + f_{jm\sigma}^\dagger f_{im\sigma}) \quad (12)$$

The free fermion hamiltonian (9) describes the quasiparticle degrees of freedom. Their effective mass is set by the renormalisation of the hopping: $t_m^{eff}/t_m = 4 \langle S_{im\sigma}^x S_{jm\sigma}^x \rangle$.

The quasiparticle weight is associated with a different quantity, namely:

$$Z_m = 4 \langle S_{im\sigma}^x \rangle^2 \quad (13)$$

Note that it depends in general on the orbital, a key feature for the physics that we want to address with this technique. Both the renormalisation of the mass and the quasiparticle weight are self-consistently determined from the solution of the quantum-spin hamiltonian (10), which describes the charge dynamics. As clear from (13), metallic behaviour for orbital m corresponds to long-range order in S_m^x , while Mott insulating behaviour corresponds to $\langle S_m^x \rangle = 0$.

At this stage, the slave-spin degrees of freedom are still described by a quantum spin hamiltonian on the lattice, and we therefore make the additional approximation (iii) of treating this model on the level of a single-site mean-field. We thus have to solve the single-site spin hamiltonian:

$$H_s = \sum_{m\sigma} 2h_m S_{m\sigma}^x + \sum_{m\sigma} \lambda_m (S_{m\sigma}^z + \frac{1}{2}) + H_{int}[\vec{S}_{m\sigma}] \quad (14)$$

in which the mean-field h_m is determined self-consistently from:

$$h_m = 2z J_m^{eff} \langle S_{m\sigma}^x \rangle \quad (15)$$

where z is the coordination number of the lattice. This equation can be combined with (12) to yield:

$$h_m = 4 \langle S_{m\sigma}^x \rangle \frac{1}{N} \sum_{\mathbf{k}} \epsilon_{\mathbf{km}} \langle f_{\mathbf{km}\sigma}^\dagger f_{\mathbf{km}\sigma} \rangle \quad (16)$$

In this expression, the fermionic expectation value is to be calculated with the quasiparticle hamiltonian (9). Within this single-site mean-field approximation however, the renormalisation of the hopping becomes identical to the quasiparticle residue since $\langle S_{im\sigma}^x S_{jm\sigma}^x \rangle$ factorizes into $\langle S_{im\sigma}^x \rangle^2$. As a result, the quasiparticle hamiltonian reads:

$$H_{eff}^f = \sum_{\mathbf{k}, m\sigma} (Z_m \epsilon_{\mathbf{km}} + \epsilon_m - \mu - \lambda_m) f_{\mathbf{km}\sigma}^\dagger f_{\mathbf{km}\sigma} \quad (17)$$

with $\epsilon_{\mathbf{km}} \equiv -t_m/z \sum_{j, n, n(i)} e^{-\mathbf{k} \cdot (\mathbf{i} - \mathbf{j})}$ the Fourier transform of the hopping. Equations (13,14,16,17) and the constraint equation (7) self-consistently determine the variational parameters h_m , λ_m and $Z_m = 4 \langle S_{m\sigma}^x \rangle^2$. They are the basic mean-field equations based on the slave-spin representation, which will be used below. Solving these equations requires to diagonalize the single-site spin hamiltonian (14), corresponding to a $4N \times 4N$ matrix.

Let us finally discuss the case of a non-zero Hund's coupling $J \neq 0$. The first three terms in (2) are easy to treat in the slave-spin formalism, since they involve only density-density interactions and are thus directly

expressed in terms of the Ising components of the slave spins. They read:

$$\frac{U'}{2} \sum_i \left(\sum_{m,\sigma} S_{im\sigma}^z \right)^2 + J \sum_{i,m} \left(\sum_{\sigma} S_{im\sigma}^z \right)^2 - \frac{J}{2} \sum_{i,\sigma} \left(\sum_m S_{im\sigma}^z \right)^2 \quad (18)$$

In contrast, the “spin-flip” and (intra-site) “pair-hopping” terms (last two terms in (2)) are more difficult to deal with, since they involve both slave-spin and auxiliary fermions operators. As a result, four-fermion terms are introduced which require additional mean-field decouplings. For simplicity, we choose to mimic the effect of these terms by replacing them by operators which have exactly the same effect on the slave-spin quantum numbers of the Hilbert space, namely:

$$\begin{aligned} & -J \sum_i \left[S_{i1\uparrow}^+ S_{i1\downarrow}^- S_{i2\downarrow}^+ S_{i2\uparrow}^- + S_{i1\downarrow}^+ S_{i1\uparrow}^- S_{i2\uparrow}^+ S_{i2\downarrow}^- \right] \\ & -J \sum_i \left[S_{i1\uparrow}^+ S_{i1\downarrow}^- S_{i2\uparrow}^- S_{i2\downarrow}^+ + S_{i2\uparrow}^+ S_{i2\downarrow}^- S_{i1\uparrow}^- S_{i1\downarrow}^+ \right], \quad (19) \end{aligned}$$

Despite the fact that these terms connect the physical and unphysical parts of the Hilbert space (and therefore would strictly vanish if the constraint was implemented exactly), it is reasonable to expect that they will qualitatively describe the physics of the spin-flip and pair-hopping terms when the constraint is treated on average, because their action on the slave-spin quantum numbers is the correct one. Hence, we shall use the following representation of the interacting part of the hamiltonian for $J \neq 0$:

$$\begin{aligned} H_{int} \approx & \frac{U'}{2} \sum_i \left(\sum_{m,\sigma} S_{im\sigma}^z \right)^2 \\ & + J \sum_{i,m} \left(\sum_{\sigma} S_{im\sigma}^z \right)^2 - \frac{J}{2} \sum_{i,\sigma} \left(\sum_m S_{im\sigma}^z \right)^2 \\ & - J \sum_i \left[S_{i1\uparrow}^+ S_{i1\downarrow}^- S_{i2\downarrow}^+ S_{i2\uparrow}^- + S_{i1\downarrow}^+ S_{i1\uparrow}^- S_{i2\uparrow}^+ S_{i2\downarrow}^- \right] \\ & - J \sum_i \left[S_{i1\uparrow}^+ S_{i1\downarrow}^- S_{i2\uparrow}^- S_{i2\downarrow}^+ + S_{i2\uparrow}^+ S_{i2\downarrow}^- S_{i1\uparrow}^- S_{i1\downarrow}^+ \right] \quad (20) \end{aligned}$$

C. Benchmarks

In this section, we perform some benchmarks of the slave-spin representation and mean-field theory.

1. Atomic limit ($J=0$)

In the $J = 0$ case we check explicitly that the atomic limit (i.e. $t_m = 0$) of the degenerate N -band model with $SU(2N)$ symmetry is correctly reproduced. Indeed our equations simplify drastically in this limit ($\tilde{t}_m = h_m = 0$), leaving only the $\lambda_{m\sigma} = \bar{\lambda}$ to be determined. The

constraint equation (7) reads in this case:

$$n_F(\mu - \bar{\lambda}) = \mathcal{Z}^{-1} \sum_{Q=0}^{2N} \mathcal{N}_Q Q e^{-\beta \left[\frac{U}{2}(Q-N)^2 + \bar{\lambda}Q \right]} \quad (21)$$

where $n_F(\epsilon)$ is the Fermi function, $\mathcal{Z} \equiv \sum_{Q=0}^{2N} \mathcal{N}_Q \exp -\beta \left[\frac{U}{2}(Q-N)^2 + \bar{\lambda}Q \right]$, $\mathcal{N}_Q \equiv \binom{2N}{Q}$ and Q is the total number of particles. Solving numerically this equation for $\bar{\lambda}$ leads to the correct “Coulomb staircase”, as shown in Fig.1, as long as $T \ll U$. At high temperatures the fact that we have imposed the constraints only in average limits the accuracy, but in practice $T \ll U$ is not a severe limitation.

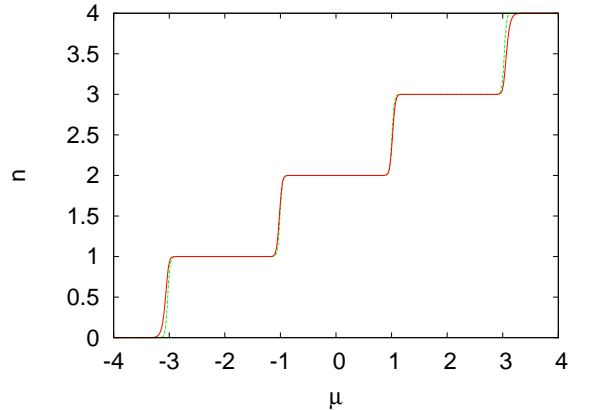


FIG. 1: Filling vs chemical potential for a two-orbitals impurity (atomic limit of a particle-hole symmetric Hubbard model), $U = 2$, $\beta = 50$: within the slave spin mean field (full line) and exact result (dashed line). The Coulomb staircase is correctly reproduced up to temperatures of order $\sim U$

2. N -orbital Hubbard model with $SU(2N)$ symmetry and large- N limit

Here, we apply the slave-spin mean-field approximation to the N -orbital model ($m = 1, \dots, N$), in the case where all bands have the same hopping, with $J = 0$. The results for the quasi-particle weight as a function of U , at half-filling, are displayed on Fig. 2. A transition into a Mott phase is found for $U > U_c(N)$. The exact large N behaviour of $U_c(N)$ in the limit of infinite coordination (DMFT) is known¹⁸ to be linear in N , the slope being $U_c/N = 8|\bar{\epsilon}|$, where $\bar{\epsilon} \equiv \int_{-\infty}^0 d\epsilon D(\epsilon)\epsilon$. This slope is correctly reproduced by the slave-spin mean-field approximation, indicating that this approximation becomes more accurate as N is increased.

One can actually calculate analytically the critical value of the coupling within this approach, for arbitrary N , by performing a perturbative expansion around the atomic limit for small h_m . This yields:

$$U_c = 8(N+1)|\bar{\epsilon}| \quad (22)$$

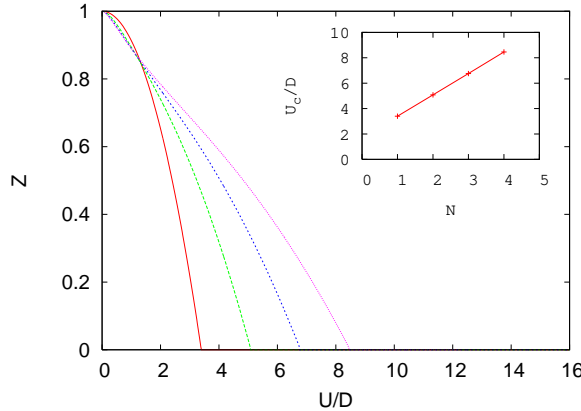


FIG. 2: Quasiparticle weight, obtained from slave-spin mean-field for the N -orbital Hubbard model at half-filling (with, from left to right: $N = 1, 2, 3, 4$). The non-interacting density of states is a semi-circle with half bandwidth D Inset: Dependence of the critical U on N . The exact large- N behaviour is obtained.

which coincides with the numerical determination in the inset of Fig. 2. We also note that (22) is precisely the result of the Gutzwiller (slave-boson) approximation in the multi-orbital case.

D. Comparison with slave bosons and slave rotors

As suggested by the fact they yield identical values of U_c , the slave-spin mean-field theory has many similarities with the Gutzwiller approximation (GA). In fact, as shown on Fig. 3, the whole dependence of Z on U is identical to that of the GA.

The slave spin representation has several advantages over the slave-boson representations that can be used to formulate the GA. One advantage is that the number of variables is smaller: $2N$ spin-1/2 degrees of freedoms instead of 2^N slave bosons (one associated to each state in the Hilbert space, in the absence of symmetries). Another advantage is that the number of unphysical states is smaller than in slave boson representations, because the Hilbert space spanned by the $2N$ quantum spins is finite by construction, while the Hilbert space associated with the slave bosons in the absence of the constraint is an infinite-dimensional one. This might be useful in considering finite-temperature properties and the entropy of the model.

A similar remark applies when comparing the present slave-spin representation to the slave-rotor representation recently developed by S. Florens and one of the authors^{16,17}. This representation is specifically tailored to $SU(2N)$ symmetric models, and is very economical since it introduces only *one* slave variable. Specifically, a (slave) quantum rotor and auxiliary fermions are intro-

duced on each site such that:

$$d_{im\sigma}^\dagger = f_{im\sigma}^\dagger e^{i\theta_i}, \quad d_{im\sigma} = f_{im\sigma} e^{-i\theta_i} \quad (23)$$

where the phase is conjugate to the local charge, corresponding to the local constraint:

$$\sum_{m\sigma} (f_{im\sigma}^\dagger f_{im\sigma} - \frac{1}{2}) = \hat{L}_i \quad (24)$$

in which $\hat{L}_i = 1/i\partial/\partial\theta_i$ is the conjugate momentum to the phase. It is clear from these expressions that there is a close similarity between the slave-spin and slave-rotor formalisms. Two important differences must be noted: (i) a single slave-rotor variable is introduced for all orbitals and (ii) the Hilbert space of the unconstrained rotor is infinite-dimensional, containing an infinite tower of charge states $|l\rangle$ which are physical only for $|l| \leq N$. As a result, mean-field approximations in which the constraint is treated only on average are less accurate when the contribution of these unphysical charge states become sizeable. This is particularly true in the weak-coupling limit. On Fig. 3, we compare the slave-spin and slave-rotor result for the quasiparticle residue in the one-band case, in order to illustrate this effect.

On the whole, slave-rotors and slave-spins offer two useful representations, the former being very economical and well suited to situations in which only the total local charge is involved (e.g in Coulomb blockade problems¹⁹), while the latter is well suited to the investigation of orbital-dependent properties, as in the present article. Both methods are easy to implement at a very low numerical cost, hence allowing for a fast and efficient investigation of the phase diagram and phase transitions in a wide range of parameters.

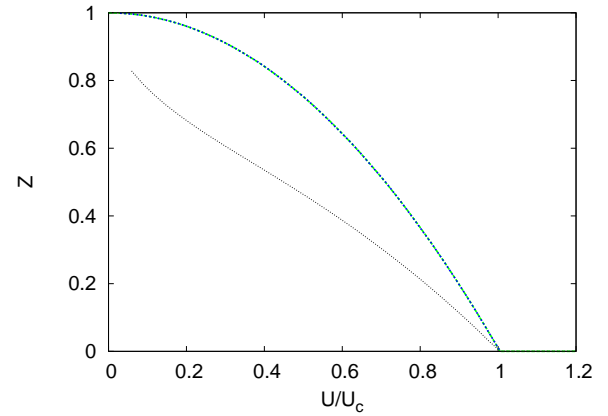


FIG. 3: Quasiparticle weight of the one-band Hubbard model, obtained with slave rotors (thin line), slave spins, and the Gutzwiller (slave boson) approximations (thick lines). The latter two actually coincide. The small- U behaviour of the slave-rotor approach is due to the larger number of unphysical states (see text).

IV. ORBITAL-SELECTIVE MOTT TRANSITION WITH SLAVE-SPIN MEAN FIELD THEORY

In this section, we use slave-spin mean-field theory in order to study the two-band model with unequal hoppings. The non-interacting density of states of each band is taken to be a semi-circle (of half-width $D_1 = 2t_1$ and $D_2 = 2t_2 < D_1$), corresponding to a Bethe lattice with infinite connectivity $z = \infty$ and nearest-neighbour hoppings $t_{1,2}/\sqrt{z}$. No crystal-field splitting is introduced ($\epsilon_1 = \epsilon_2 = 0$) and we restrict ourselves to the case in which both bands are half-filled ($\langle n_1 \rangle = \langle n_2 \rangle = 1$). The model is thus particle-hole symmetric, implying that the chemical potential $\mu = 0$ and Lagrange multipliers $\lambda_1 = \lambda_2 = 0$. The parameter space was explored for $U > 0$, $J = 0 \div 0.5U$ i.e. $U' = U - 2J = 0 \div U$, and the ratio between the two bandwidths $t_2/t_1 = 0 \div 1.0$. For the study of the Mott transitions in this model we monitor the quasiparticle weights $Z_m = 4\langle S_{m\sigma}^x \rangle^2$.

Fig. 4 displays the phase diagram within slave-spin mean-field theory for the bandwidth ratio $t_2/t_1 = 0.5$. Three different phases are found: at small U both bands are metallic (i.e. $Z_m \neq 0$), at large U both are insulating ($Z_m = 0$), and in between an “orbital selective Mott phase” (OSMP) is found in which only the band with largest bandwidth has $Z_1 \neq 0$, while the narrower band has $Z_2 = 0$.

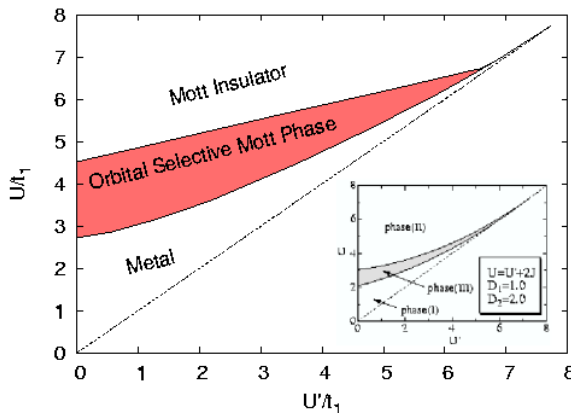


FIG. 4: Phase diagram (U vs U') for $t_2/t_1 = 0.5$ at $T = 0$ within the Slave Spins mean field theory. Inset, same diagram obtained with Exact diagonalization-Dynamical Mean Field Theory (ED-DMFT) in⁹. The dotted line indicates $J = 0$, i.e. $U = U'$. In “phase I” both bands are metallic, in “phase II” both bands are insulating. “Phase III” is the orbital-selective Mott phase.

In the inset of Fig. 4, we reproduce for comparison the result of Koga *et al.*⁹) obtained within DMFT. Qualitatively, one sees that the slave-spin mean-field compares rather well to the DMFT results. There are quantitative differences in the critical values of the couplings U and U' , a well known feature of Gutzwiller-like approximations. Also, the linear dependence on U' of the upper

boundary of the OSMP phase is due to the simplified treatment of the spin-flip and pair-hopping terms discussed above (as indeed confirmed by the results of section IV C).

There is however one significant qualitative difference between the slave-spin results and those of Koga *et al.* (inset). We find that the endpoint of the OSMP phase *does not lie exactly on the $U = U'$ line*. Hence, within the slave-spin mean field, the Mott transition becomes orbital-selective (OSMT) only when J exceeds a critical value. This is a rather significant finding, since for $J = 0$ the interacting part of the hamiltonian (H_{int}) has full $SU(4)$ spin-orbital symmetry, while for $J \neq 0$ the symmetry is lower. In Ref.⁹, it was argued that indeed the enhanced symmetry of the $J = 0$ case prevents an orbital-selective Mott transition to occur. Our finding that a critical value of J is needed to induce an OSMT (for $t_2/t_1 = 0.5$) suggests that symmetry considerations on H_{int} may not be essential to the existence of an orbital-selective transition. After all, the difference in bandwidths breaks the $SU(4)$ symmetry from the kinetic energy part of the hamiltonian. In order to study this issue in more detail, we perform in the next section a detailed study of the $J = 0$ case.

A. OSMT at $J = 0$

In this section, we focus on the $J = 0$ case, for which H_{int} has full $SU(4)$ symmetry, and explore the nature of the Mott transition in the full range of bandwidth ratio from $t_2/t_1 = 0$ to $t_2/t_1 = 1$.

We find that the two bands undergo a common Mott transition at a single value of $U = U_c$ as long as the bandwidth ratio exceeds a critical threshold: $t_2/t_1 > 0.2$. In contrast, for $t_2/t_1 < 0.2$, *an orbital-selective Mott phase is found*, despite the enhanced symmetry of the interaction term. Fig. 4 displays our result for the phase diagram as a function of t_2/t_1 and U/t_1 . All transitions are found to be second-order when $J = 0$. On Fig. 5, the quasiparticle weights of each band is plotted as a function of U , for several values of t_2/t_1 . The localization of the narrower band manifests itself as a kink in the quasiparticle weight of the wider band. As U is increased further, the wide band in turn undergoes a Mott transition. We observe that, within slave-spin mean-field, the quasiparticle weight of the wider band in the orbital-selective Mott phase coincides with that of a single-band model. This is because the slave-spin mean-field neglects charge fluctuations of the localised orbital, so that the physical behavior of the wide band becomes effectively that of a one-band model as soon as the narrow band becomes localized.

Our finding of an orbital-selective Mott transition at $J = 0$ when t_2/t_1 is small enough, within slave-spin mean-field theory, raises two questions. First, is this finding an artefact of the slave-spin approximation or does it survive a full DMFT treatment (i.e. is it a genuine fea-

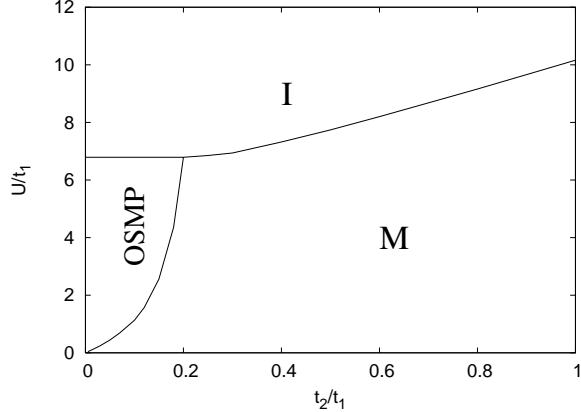


FIG. 5: Dependence of the critical U on the ratio t_2/t_1 at $J = 0$ and $T = 0$. All transitions are second-order.

ture of the infinite-coordination model ?). Second, does this invalidate the argument based on the symmetry of H_{int} ? The first question will be addressed in detail in Sec. V, in which a DMFT study will be performed, using exact diagonalization and Quantum Monte-Carlo techniques. We will show that indeed, a transition does exist at $J = 0$ when t_2/t_1 is small enough, but that the nature of the intermediate phase (OSMP) at low-energy is a rather subtle issue. In order to address the second question, let us briefly recall the symmetry argument of Koga *et al.*⁹. The argument relies on the gap to charge excitations in the insulating phase. When $J = 0$, charge excitations mix the two orbitals because of the enhanced $SU(4)$ symmetry. Instead, for $J \neq 0$, the charge excitations of lowest energy are independent in each orbital sector. As a result, it is reasonable to expect (at least when the kinetic energy term is treated in a perturbative manner) that the system can sustain two different charge gaps when $J \neq 0$ while the gaps might coincide for $J = 0$. We observe however that this argument applies to the instability of the large- U Mott phase (in which both bands are gapped) when U is reduced, and suggests that, for $J = 0$, the Mott gap closes at the same value of U for both bands when U/t_1 is reduced. It does not preclude however that a transition into an intermediate phase does exist, in which the ‘‘localised’’ band (with the narrower bandwith) is not fully gapped. As we shall find below, there is indeed clear evidence from the DMFT results that the orbital-selective Mott phase at $J = 0$ is *not a conventional Mott insulator* and that the narrow (‘‘localised’’) band does have spectral weight down to zero-energy in this phase. Obviously, the slave-spin mean-field approach is too rudimentary to be able to capture these fine low-energy aspects, but it is remarkable that it does allow us to infer correctly that an intermediate phase is indeed present.

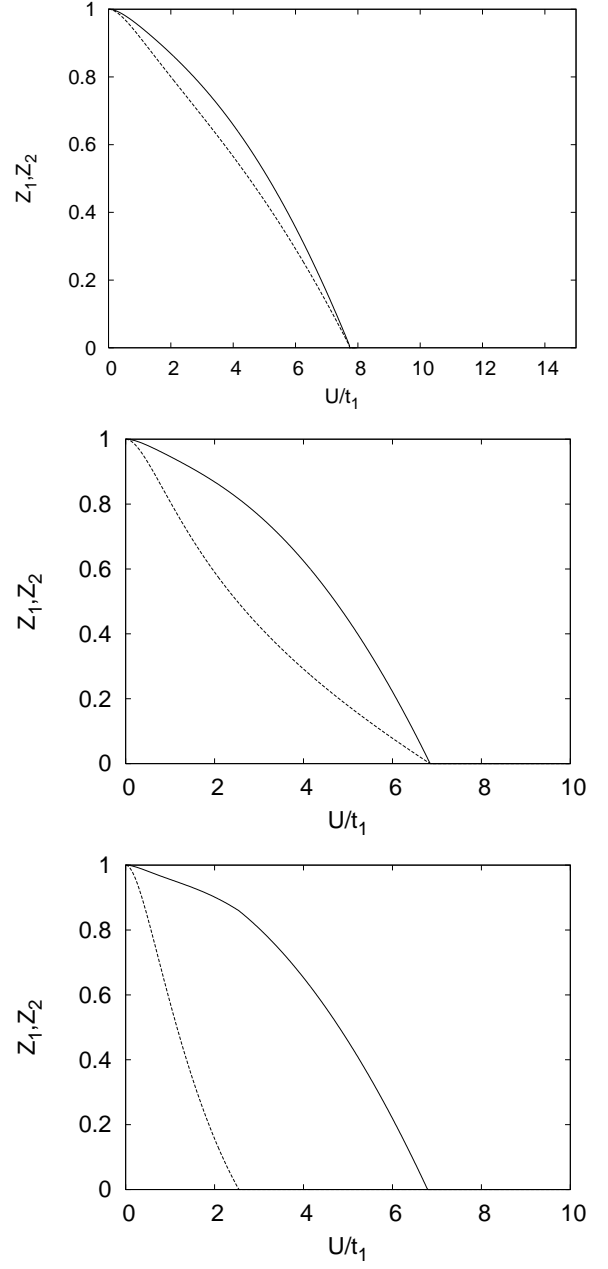


FIG. 6: Z_m at $J = 0$ and $T = 0$ for $t_2/t_1 = 0.5$ (top), 0.25 (middle), 0.15 (bottom).

B. Dependence of OSMT on J

Having clarified the situation for $J = 0$, we come back to the effect of a non-zero J , still within the slave-spin mean-field approximation. Fig. 7 shows how the phase diagram as a function of the bandwidth ratio t_2/t_1 and of U/t_1 is modified for $J \neq 0$. One sees that a finite J enlarges the orbital-selective Mott phase and favors an OSMT. The critical ratio $(t_2/t_1)_c$ below which an OSMP exists increases significantly, e.g. $t_2/t_1 \simeq 0.55$ for $J = 0.01U$. With increasing J , $(t_2/t_1)_c$ tends towards 1.

Hence a common Mott transition for both bands is recovered for all values of J only when $t_1 = t_2$. For a given bandwidth ratio t_2/t_1 , the Mott transition is orbital-selective for $J/U > (J/U)_c$. The dependence of this critical ratio upon t_2/t_1 (i.e the location of the endpoint of the OSMP phase) is displayed in Fig. 8. (It should be noted however that this critical ratio $(J/U)_c$ is underestimated by our simplified treatment of the pair-hopping and spin-flip term). Finally, we found that for finite J , the insulator to OSMP transition remains second-order, while the metal to OSMP transition becomes first-order.

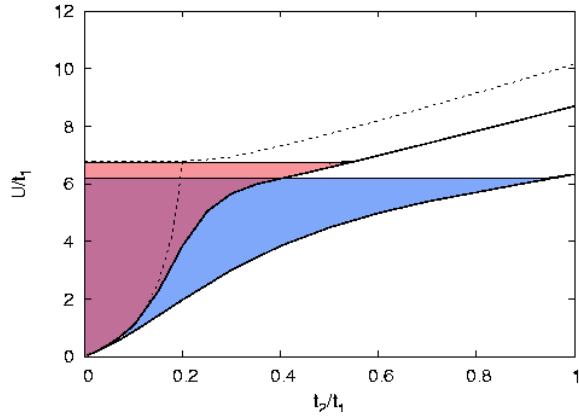


FIG. 7: Widening of the OSMT zone with increasing J/U at $T = 0$. Transition lines are shown for (from left to right) $J/U = 0$ (dashed), 0.01, 0.1

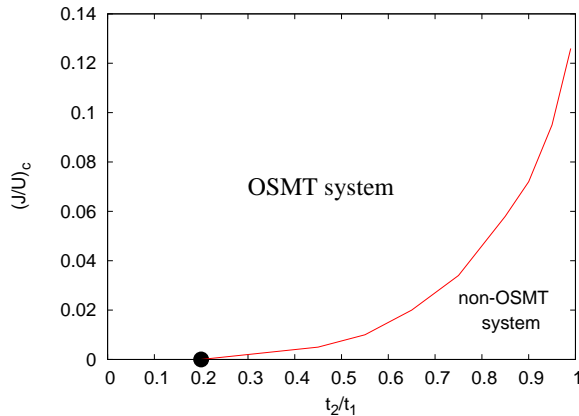


FIG. 8: Dependence of the critical J/U above which the Mott transition becomes orbital-selective, on the ratio t_2/t_1 at $T = 0$.

C. Role of the spin-flip and pair-hopping terms in the Hund Hamiltonian

In order to clarify the role played by the different terms of the interaction (2), we have also studied the Hamilto-

nian in which the spin-flip and the (on-site) inter-orbital pair-hopping terms are dropped, namely:

$$H_{int} = U \sum_{im} \tilde{n}_{im\uparrow} \tilde{n}_{im\downarrow} + (U - 2J) \sum_{i\sigma} \tilde{n}_{i1\sigma} \tilde{n}_{i2\sigma} + (U - 3J) \sum_{i\sigma} \tilde{n}_{i1\sigma} \tilde{n}_{i2\sigma}. \quad (25)$$

which is easily represented in terms of slave-spins as:

$$H_{int} = \frac{U'}{2} \sum_i \left(\sum_{m,\sigma} S_{im\sigma}^z \right)^2 + J \sum_{i,m} \left(\sum_{\sigma} S_{im\sigma}^z \right)^2 - \frac{J}{2} \sum_{i,\sigma} \left(\sum_m S_{im\sigma}^z \right)^2 \quad (26)$$

This study is also motivated by a comparison to Quantum Monte-Carlo treatments in which the spin-flip and pair-hopping terms are not easily treated. On Fig. 9 we display the slave-spin phase diagram found for $t_2/t_1 = 0.5$ at zero-temperature. One sees that the OSMP shrinks dramatically (albeit the two transitions do not actually merge). This finding sheds light on the recent claim by Liebsch that the orbital-selective Mott transition is actually absent^{7,8,10}. Because this study was based on Quantum-Monte Carlo, hence neglecting the spin-flip and inter-orbital pair-hopping terms, it is natural that the orbital-selective phase can be found only in a very narrow range of parameter space. The key role of spin-flip and inter-orbital pair-hopping terms for the OSMT was actually pointed out in the recent work of Koga et al.¹¹.

In Fig. 10, we display the region in $t_2/t_1, J/U$ parameter space where the Mott transition is found to be orbital-selective, analogously to Fig. 8. The critical ratio $(J/U)_c$ is found to be roughly exponential in t_2/t_1 . In contrast to the case of the full hamiltonian (Fig. 8), we find that no OSMT exists when t_2/t_1 exceeds a critical bandwidth ratio $t_2/t_1 \simeq 0.6$, for any J/U . Beyond this value no OSMT is found at any J/U . (Note that the upper critical line at large J/U corresponds however to the unphysical case of an attractive Coulomb interaction due to $U - 3J < 0$).

Finally, we emphasize that the orbital-selective Mott phase, which exists only in a very narrow range of couplings for the simplified interaction (25) at $T = 0$, is actually enlarged at finite-temperature, as shown in Fig. 11.

V. DYNAMICAL- MEAN FIELD THEORY FOR $J = 0$ AND NATURE OF THE OSMT PHASE

In this section, we study the two-band model with $J = 0$ using dynamical mean-field theory. Our goal is to determine whether the transition into an orbital-selective Mott phase (OSMP) found within the slave-spin approximation at small enough t_2/t_1 is indeed a robust feature, and to shed light on the possible low-energy physics of this phase. Within DMFT, the lattice model is

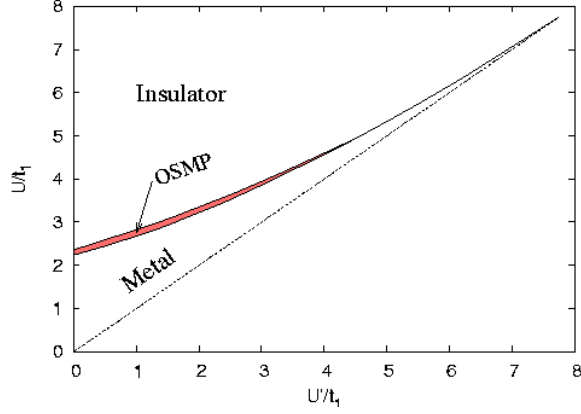


FIG. 9: Phase diagram (U vs U') for $t_2/t_1 = 0.5$ at $T = 0$ for a two-band Hubbard model without spin flip and pair hopping terms in the interaction.

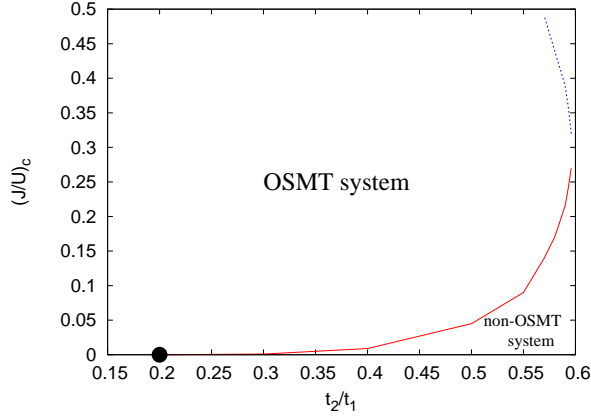


FIG. 10: Critical J/U for the model without spin-flip and pair-hopping as a function of t_2/t_1 . At small ratios of the bandwidths, the system displays an OSMT above a critical J/U ratio which vanishes at $t_2/t_1 = 0.2$. In less anisotropic systems large Hund's coupling are needed to realize OSMPs, whereas beyond the critical bandwidth ratio of 0.6 no OMST is possible within this model.

mapped onto a self-consistent two-orbital Anderson impurity model^{1,20} with effective action:

$$-\int_0^\beta \int_0^\beta d\tau d\tau' \sum_{m\sigma} d_{m\sigma}^\dagger(\tau) \mathcal{G}_m^{-1}(\tau - \tau') d_{m\sigma}(\tau') + \frac{U}{2} \int_0^\beta d\tau (n_1 + n_2 - 2)^2 \quad (27)$$

The hybridisations to the effective conduction bath are self-consistently related to the local interacting Green's functions G_m through:

$$\mathcal{G}_m(i\omega_n)^{-1} = i\omega_n - t_m^2 G_m(i\omega_n) \quad (28)$$

These equations are exact for an infinite-connectivity Bethe lattice (corresponding to semi-circular non-interacting d.o.s). Particle-hole symmetry with one electron per site in each band has been assumed. We focus here on the paramagnetic solutions only. The DMFT

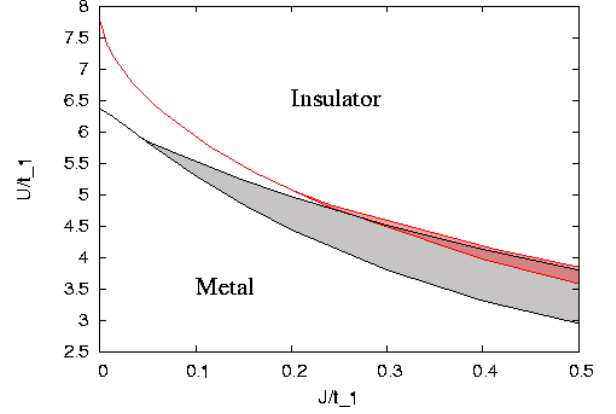


FIG. 11: Same phase diagram as in fig. 9 but in the U - J plane at $T = 0$ and at $\beta t_1 = 40$.

equations will be solved in the following using both an exact diagonalisation (ED) and Quantum Monte-Carlo (QMC) technique.

A. Exact diagonalisation study

Within the adaptative exact-diagonalization method^{1,21}, the effective conduction-electron bath is discretized using a finite number of orbitals N_s . Hence, one considers the two-orbital Anderson impurity hamiltonian:

$$H_{AIM} = \sum_{m\sigma} \sum_{l=1}^{N_s} \epsilon_{lm} a_{lm\sigma}^\dagger a_{lm\sigma} + \sum_{m\sigma} \sum_{l=1}^{N_s} V_{lm} (d_{m\sigma}^\dagger a_{lm\sigma} + h.c.) + \frac{U}{2} (\hat{n}_1 + \hat{n}_2 - 2)^2 \quad (29)$$

The operators $a_{lm\sigma}, a_{lm\sigma}^\dagger$ describe the discretized conduction- bath degrees of freedom. The effective parameters $\{\epsilon_{lm}, V_{lm}\}$ have to be determined self-consistently, according to (28), namely:

$$\sum_{l=1}^{N_s} \frac{|V_{lm}|^2}{i\omega_n - \epsilon_{lm}} = t_m^2 G_m(i\omega_n) \quad (30)$$

The ED method becomes an asymptotically exact solver of the DMFT equations in the limit $N_s \rightarrow \infty$. In practice however, one can handle only a finite number of effective sites. For the case at hand, we used a $T = 0$ Lanczos algorithm, with $N_s = 5$ (i.e 5 effective sites per orbital). The self-consistency (30) is implemented on a Matsubara grid corresponding to a (fictitious) inverse temperature β (taken to be in practice in the range 200 to 500, which insures a good resolution on the low-energy physics). We monitor in particular the quasiparticle weights, approximated as: $Z_m = [1 - \text{Im}\Sigma_m(i\omega_0)/\omega_0]^{-1}$ (where $\omega_n = \pi/\beta(2n + 1)$).

Our ED results for these quantities are displayed on Fig. 12, and compared to the slave-spin results, both as a function of U for fixed t_2/t_1 and as a function of t_2/t_1 for fixed U (inset). It is clear from this figure that, within the energy resolution which can be reached with $N_s = 5$, an orbital-selective transition is indeed observed in the DMFT(ED) results when t_2/t_1 is smaller than a critical value (close to 0.25), in remarkable agreement with the slave-spin mean-field. The quantitative value of the critical coupling U/t_1 for the localisation of the wider band is overestimated, as usual in Gutzwiller-like schemes.

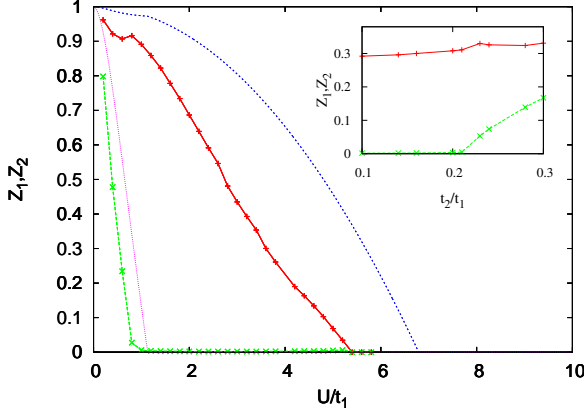


FIG. 12: Quasiparticle residues at $J = 0$ in DMFT(ED) for $t_2/t_1 = 0.1$ (symbols). For comparison, the slave-spin mean-field approximation is also displayed (continuous line). Inset: same quantities as a function of t_2/t_1 at fixed $U/t_1 = 4.0$. (The kinks in Z_1 are associated with the criticality of Z_2).

The phase diagram obtained with ED, as a function of t_1/t_2 and U/t_1 is displayed in Fig. 13. Good qualitative agreement with the slave-spin mean field is found (Fig. 5). We also studied the hysteresis properties by performing runs for increasing and decreasing values of U/t_1 . This results in two almost parallel transition lines on Fig. 13, one corresponding to the disappearance of the metallic solution (obtained from a series of runs for increasing U), the other corresponding to the loss of the insulating nature of the wide band (from a series of runs for decreasing U). In the region between these two lines, coexistence of two types of DMFT solutions is found: for small t_2/t_1 , one of the solutions is orbital-selective Mott and the other is fully insulating, while for larger t_2/t_1 , one of the solutions is metallic and the other fully insulating. The actual thermodynamic transition is given by the crossing of the free energies of the two solutions. In contrast, no hysteresis has been found at the transition between the OSMP and metallic phases. This suggests that the transition from the metallic to the OSMP phase is of a very different nature than the Mott transition of the wider band. If only the gap closure is monitored, then only one transition is found at $J = 0$, in agreement with the symmetry argument of Ref.⁹. As we shall demonstrate below, there is indeed strong evidence that the orbital-selective Mott phase at $J = 0$ does not display

a sharp gap in either orbitals.

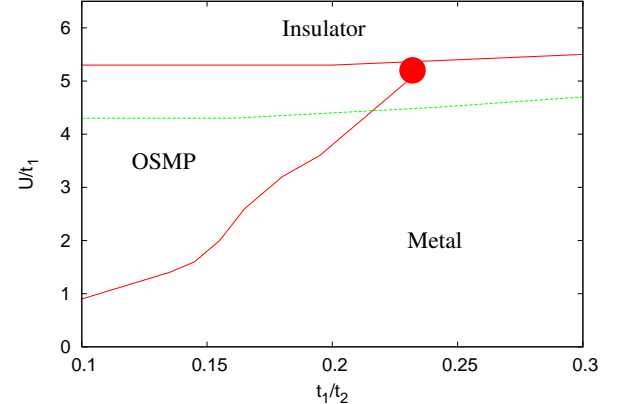


FIG. 13: Phase diagram at $J = 0$ and $T = 0$ in ED-DMFT. The dashed line marks the disappearance of the Mott gap (downward runs). For U values around 5 there is coexistence between an OSMP and - depending on the bandwidth ratio - an insulating or metallic phase.

B. Low-energy nature of the orbital-selective Mott phase at $J = 0$, from ED and QMC

In order to understand better the nature of the orbital-selective phase found at $J = 0$, we take a closer look at the local Green's function for each orbital, in each phase. In order to do this, we also solved the DMFT equations using the Quantum Monte-Carlo algorithm of Hirsch and Fye²². The ED and QMC methods are quite complementary. The former applies at $T = 0$ but suffers from a limited energy- resolution due to the small value of N_s , while the latter is limited to finite-temperature but can be made very precise by increasing the number of time slices and the number of Monte-Carlo sweeps (we used 128 slices in imaginary time and up to 5×10^5 Monte Carlo sweeps in practice). Also, using QMC allows for a reconstruction of the spectral functions using a numerical analytic continuation based on the maximum entropy algorithm.

In Fig. 14, we display the ED results for the local Green's functions on the Matsubara axis, for a small bandwidth ratio t_2/t_1 and three different values of U corresponding to the insulating, metallic, and orbital-selective Mott phases. In the particle-hole symmetric case, the Green's functions are purely imaginary on the Matsubara axis and related to the spectral function $A_m(\epsilon)$ of each orbital by:

$$\text{Im}G_m(i\omega) = -2\omega \int_0^{+\infty} d\epsilon \frac{A_m(\epsilon)}{\omega^2 + \epsilon^2} \quad (31)$$

When the spectral function $A_m(\epsilon)$ has a gap, the integral in the right-hand side of (31) has no singularity in the $\omega \rightarrow 0$ limit, and hence $\text{Im}G_m(i\omega) \propto \omega$ at low

frequency. Furthermore, $\text{Im}G_m(i\omega)$ has a minimum for ω of order $\Delta_m/2$, with Δ_m the gap in the m -th orbital (as can be seen by replacing $A_m(\epsilon)$ by the simplified form $1/2[\delta(\epsilon - \Delta_m/2) + \delta(\epsilon + \Delta_m/2)]$, yielding $\text{Im}G_m(i\omega) \simeq -2\omega/(\omega^2 + \Delta_m^2/4)$). This is fully consistent with the ED results in the upper panel of Fig. 14, corresponding to a large value of $U/t_1 = 7$, with both orbitals insulating and having a gap of order U .

In the lower panel of Fig. 14, ED results are displayed for $U/t_1 = 2$, when both orbitals are metallic. In this case, the low-frequency limit of (31) yields: $\text{Im}G_m(i\omega \rightarrow 0) = -\pi A_m(0)$. This is consistent with the numerical results, which also show that the Luttinger theorem is obeyed for both bands: $\pi A_m(0) = 1/t_m$.

The central panel of Fig. 14 displays the ED results for an intermediate coupling, corresponding to the orbital-selective phase. One sees that the wider band has metallic behaviour, with $A_1(\omega)$ still reaching the Luttinger value at $\omega = 0$. In contrast, $\text{Im}G_2(i\omega)$ appears to vanish as $\omega \rightarrow 0$, within the energy resolution of ED. However, in striking contrast to the upper panel (insulating phase), the minimum in $\text{Im}G_2(i\omega)$ is at a *very low frequency scale* which is obviously not given by U . This strongly suggests that $A_2(\omega)$ displays low-energy peaks very close to $\omega = 0$, and may even have spectral weight down to arbitrary low frequency.

Figure 15 compares the ED and QMC results for $\text{Im}G_{1,2}(i\omega)$ in the strongly anisotropic case $t_2/t_1 = 0.1$ for a relatively small Coulomb interaction $U/t_1 = 1.6$, easier to study with QMC. These parameters also correspond to the orbital-selective phase (Fig. 13). Very good agreement between the two methods is found, confirming the above analysis (and confirming also the Luttinger value for the wider band with greater accuracy than in ED). The corresponding spectral functions obtained by the maximum-entropy method are displayed on Fig. 16. The spectral function of the broader band is only slightly modified as compared to the non-interacting d.o.s. Small shoulders are visible, at the position of the lower and upper Hubbard bands, the Luttinger theorem is obeyed, and some of the spectral weight is transferred to higher energies as expected. The narrow-band however is obviously in a strong-coupling regime, with well-marked upper and lower Hubbard bands. The most striking features however are the two narrow peaks at low-frequency, which can be interpreted either as a split quasi-particle resonance or as the sign of a *pseudo-gap* (partially filled by thermal excitations since the QMC calculation is for $T/t_1 = 1/40$).

Hence, the general conclusion of this analysis is that the orbital-selective phase found for $J = 0$ at small enough t_2/t_1 is not a conventional Mott phase in which the (“localized”) orbital with narrower bandwidth would display a sharp gap. Instead, two narrow peaks exist near $\omega = 0$ and finite spectral weight is found down to low-energy. Our numerical data are consistent with a pseudo-gap behaviour, but a precise characterization of the low-energy nature of the phase will require fur-

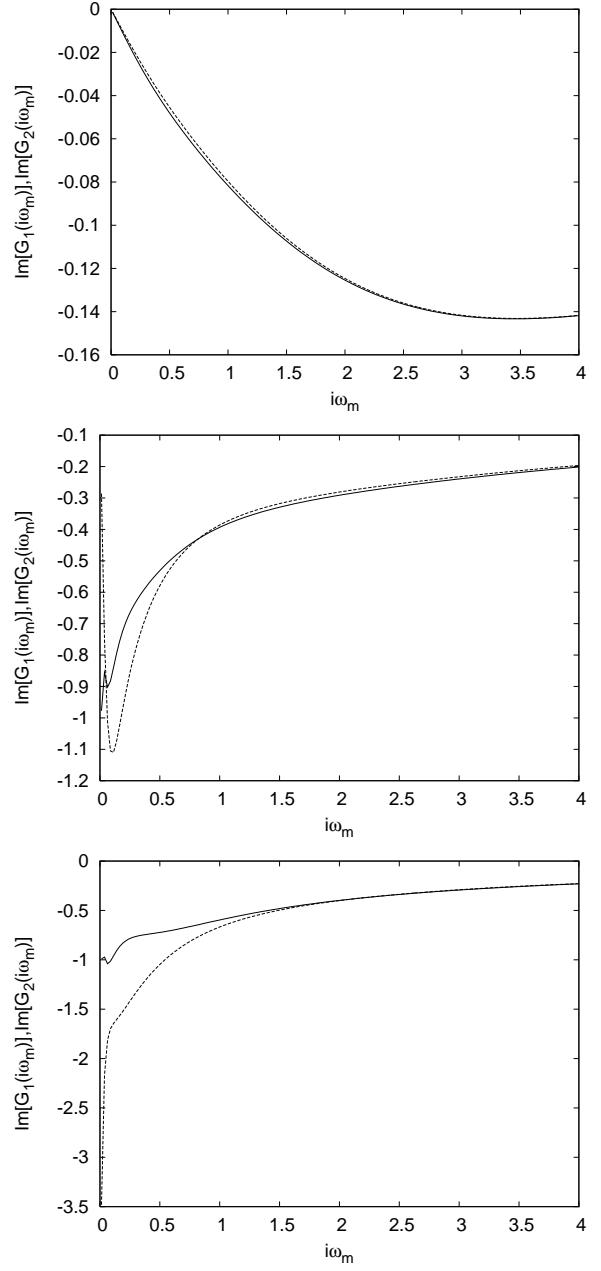


FIG. 14: Imaginary part of the Green functions of the two bands at low energy for $t_2/t_1 = 0.16$. Upper panel: $U/t_1 = 7.0$, both bands are insulating. Central panel: $U/t_1 = 4.0$, Orbital Selective Mott phase. Lower panel: $U/t_1 = 2.0$, both bands metallic. The dashed curves correspond to the orbital with narrower bandwidth. All energy scales are in units of t_1 .

ther effort, using highly precise techniques at low-energy such as the numerical renormalization group. This is left for future work. Such a study should also clarify in which precise sense the narrower band is “localized” in this phase, and whether the orbital-selective transition is a true phase transition or rather a sharp crossover.

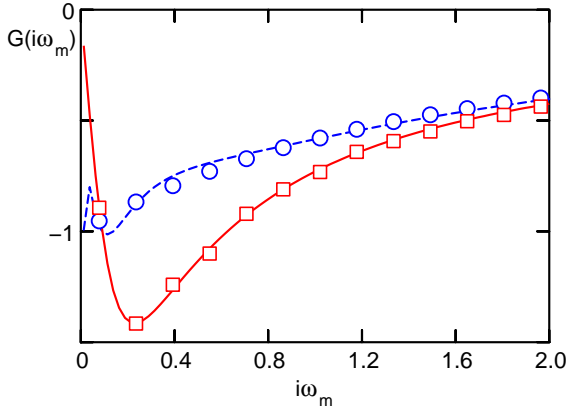


FIG. 15: Imaginary parts of the Green's functions in Matsubara space for $t_2/t_1 = 0.1$, $U/t_1 = 1.6$. Solid and dashed lines represent the exact diagonalization results for the wide and narrow bands respectively. Circles and squares represent QMC data for the same quantities at $\beta t_1 = 40$.

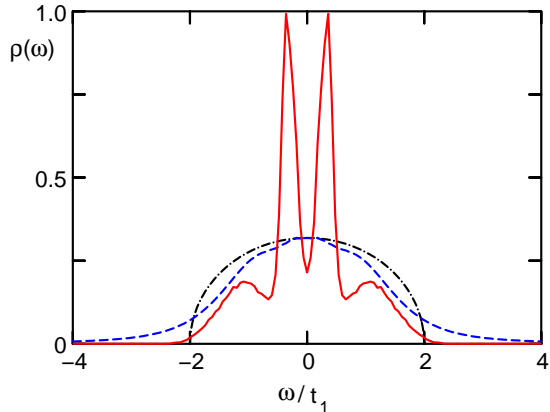


FIG. 16: Spectral function for $t_2/t_1 = 0.1$, $U/t_1 = 1.6$ at $\beta t_1 = 40$ in QMC-DMFT. The solid and dashed red lines denote the narrow and wide bands respectively. The DOS of the non-interacting system (wide band only) is given for comparison.

VI. INSTABILITY OF THE ORBITAL-SELECTIVE MOTT PHASE UPON INTER-BAND HYBRIDIZATION

To what extent an orbital-selective Mott phase may occur in practice depends on its stability with respect to perturbations. This is an important issue in view of the fact that the hamiltonian considered in this paper has a rather high degree of symmetry. In this last section, we consider the effect of an hybridization between the two orbitals, i.e of a local non-diagonal term:

$$H_{hyb} = V \sum_{i\sigma} (d_{i1\sigma}^\dagger d_{i2\sigma} + d_{i2\sigma}^\dagger d_{i1\sigma}) \quad (32)$$

We note that this term could be eliminated by diagonalizing the non-interacting hamiltonian. However, in the

new basis, the interaction terms will be modified: terms will be generated which will have the same physical effect than a hybridisation (and will involve non-local contributions in general). Indeed, as emphasized in Ref.²³, the existence of an OSMT is a *basis- independent* issue. In a general two-band model, a Mott transition is signaled, when approached from the metallic side, by a low-frequency singularity in $\omega \hat{I} - \hat{\Sigma}(\omega) = \hat{Z}^{-1}\omega + \dots$, where $\hat{\Sigma}$ and \hat{Z} are the self-energy and quasiparticle-weight matrices, respectively. An OSMT is characterized by \hat{Z} having one zero-eigenvalue while the other one remains finite. Being associated with the rank of the \hat{Z} -matrix, it is a basis-independent notion. Our choice of basis is such that the interaction terms have the form specified above.

We have studied the effect of a finite hybridization (32) using the slave-spin mean-field approximation. The results in Fig. 17 show that the hybridization is a singular perturbation on both the $J = 0$ and finite- J orbital-selective Mott phases. Any finite V induces an instability of these phases towards either the metallic (at small U) the Mott insulating phase (at large U). The two separate Mott transitions are replaced by a non selective, first order transition taking place at some U_c which lies in between the critical interactions of the metal-OSMP and OSMP-insulator transitions. The orbital-selective Mott phase is replaced by a heavy- fermion regime, as shown in Fig. 17, in which the orbital with narrower bandwidth acquires a very large effective mass (and hence is associated with a very low quasiparticle coherence scale). This is also in qualitative agreement with our recent study of the periodic Anderson model with direct f-electron hopping²³. Of course, at intermediate temperature (above the quasiparticle coherence scale of the narrower band, but below that of the wider band), a physics similar to the orbital-selective Mott phase will be recovered nevertheless.

VII. CONCLUSION

In this article, we have studied whether the Mott transition of a half-filled, two-orbital Hubbard model with unequal bandwidths occurs simultaneously for both bands or whether it is a two-stage process in which the orbital with narrower bandwidth localizes first (giving rise to an intermediate ‘orbital-selective’ Mott phase). In order to study this question, we have used two techniques. The first is a mean-field theory based on a new representation of fermion operators in terms of slave quantum spins. This method is similar in spirit to the Gutzwiller approximation, and the slave-spin representation has a rather wide range of applicability to multi-orbital models. The second method is dynamical mean-field theory, using exact diagonalization and Quantum Monte-Carlo solvers.

The results of the slave-spin mean-field confirms several aspects of previous studies^{9,11}, and in particular the possibility of an orbital-selective Mott transition (in contrast to the claims of Refs.^{7,8,10}). However, some of the

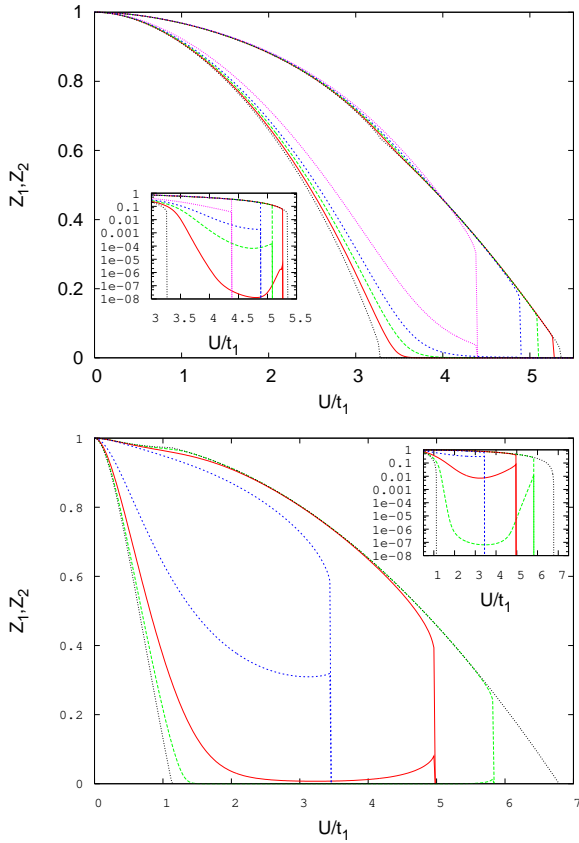


FIG. 17: Quasiparticle residues within Slave Spins - finite V on the OSMT phases. Top: $t_2/t_1 = 0.5, J = 0.25U$ for (from right to left in the upper manifold - wide band -, viceversa in the lower manifold - narrow band) $V = 0, (\text{OSMT system}), V/t_1 = 0.1, 0.15, 0.2, 0.3$ (heavy fermion regimes). Bottom: $t_2/t_1 = 0.1, J = 0$ for (from right to left in the upper manifold - wide band -, viceversa in the lower manifold - narrow band) $V = 0, (\text{OSMT system}), V/t_1 = 0.05, 0.1, 0.2$ (heavy fermion regimes). Insets show the same graph in log scale.

conclusions differ from those of previous work. Specifically, the slave-spin approximation suggests that a critical value of the bandwidth ratio $(t_2/t_1)_c$ exists, such that the Mott transition is orbital-selective for arbitrary value of the Coulomb exchange (Hund coupling) J when $t_2/t_1 < (t_2/t_1)_c$. When $t_2/t_1 > (t_2/t_1)_c$, J has to be larger than a finite threshold for an OSMT to take place.

This suggests that the existence of an OSMT is not simply related to the symmetry of the interaction term only. In particular, an intermediate phase is found for $J = 0$ at small t_2/t_1 .

We have studied whether DMFT confirms these findings, and found that the main qualitative conclusions on the existence of the orbital-selective phase are indeed the same, but that the nature of the intermediate phase at $J = 0$ is a rather subtle issue. Indeed, the narrow band does not have the properties of a gapped Mott insulator in this phase and displays finite spectral weight down to arbitrary low-energy. This is, for example, consistent with a pseudo-gap behaviour but requires further studies to be fully settled (using e.g low-energy techniques such as the numerical renormalization group).

We note also that our study emphasizes the key role of the exchange and (on-site) inter-orbital pair hopping terms in the Coulomb hamiltonian in stabilizing the orbital-selective phase, in agreement with Koga et al.¹¹.

Finally, we found that the orbital-selective Mott phase is generically unstable with respect to an inter-orbital hybridization. When such a term exists, the narrow orbital acquires a large, but finite, effective mass. Of course, at intermediate temperature (above the quasiparticle coherence scale of the narrower band, but below that of the wider band), a physics similar to the orbital-selective Mott phase will be recovered nevertheless. This orbital-selective heavy-fermion state could indeed be relevant to the physics of $\text{Ca}_{2-x}\text{Sr}_x\text{RuO}_4$.

Acknowledgments

During the completion of this paper, we learned of the work by M. Ferrero, F. Becca, M. Fabrizio and M. Capone, reaching similar conclusions. We are grateful to F. Becca, M. Fabrizio and M. Capone for discussions. A.G acknowledges discussions with S. Florens and N. Dupuis on the slave-spin representation, at an early stage of this work. We are grateful to A. Lichtenstein for help with ED calculations in the multi-orbital context. We also thank A. Koga, N. Kawakami, G. Kotliar, T.M. Rice and M. Sigrist for useful discussions. This research was supported by CNRS and Ecole Polytechnique and by a grant of supercomputing time at IDRIS Orsay (project 051393).

¹ A. Georges, G. Kotliar, W. Krauth, and M. J. Rozenberg, *Reviews of Modern Physics* **68**, 13 (1996).

² A. Georges, in *Lectures on the physics of highly correlated electron systems VIII*, edited by A. Avella and F. Mancini (American Institute of Physics, 2004), cond-mat/0403123.

³ G. Kotliar and D. Vollhardt, *Physics Today* **March 2004**, 53 (2004).

⁴ A. Georges, S. Florens, and T. A. Costi, *Journal de*

Physique IV - Proceedings **114**, 165 (2004), cond-mat/0311520.

⁵ V. Anisimov, I. Nekrasov, D. Kondakov, T. Rice, and M. Sigrist, *Eur. Phys. J. B* **25**, 191 (2002).

⁶ Z. Fang, N. Nagaosa, and K. Terakura, *Phys. Rev. B* **69**, 045116 (2004).

⁷ A. Liebsch, *Europhysics Letters* **63**, 97 (2003).

⁸ A. Liebsch, *Phys. Rev. B* **70**, 165103 (2004).

